



Cite this: *RSC Appl. Polym.*, 2025, **3**, 1385

## Organic solvent-free gelation of syndiotactic-rich poly(vinyl alcohol)

Yusuke Taoka <sup>a,b</sup> and Kazuaki Matsumura <sup>\*a</sup>

Poly(vinyl alcohol) (PVA) is commonly used in a wide variety of applications due to its desirable characteristics. However, limitations exist regarding its solubility and mechanical properties. To address this, the gelation of syndiotactic-rich polyvinyl alcohol (sPVA) with a regular three-dimensional structure was performed using an organic solvent-free approach. The obtained sPVA exhibited a higher crystallinity than the commonly used atactic PVA (aPVA). However, both systems exhibit low solubilities in solvents such as water and dimethyl sulfoxide due to their high crystallinities, thereby rendering it impossible to exploit their properties. However, since the hot pressing method does not require the dissolution of PVA in a solvent, it is possible to perform gelation using sparingly soluble materials such as sPVA. Consequently, a hydrogel was formed by applying the hot pressing method to water-swollen sPVA. The obtained sPVA hydrogel (sPVA-H) was subsequently dried and heat-treated at different temperatures to compare its crystallinity and thermal and mechanical properties with those of the aPVA hydrogel (aPVA-H). It was found that sPVA-H exhibited comparable properties to the original sPVA-H following heat treatment at higher temperatures, and also when heat-treated at a temperatures lower than those required for aPVA-H. The obtained results indicated that sPVA-H exhibits excellent mechanical properties, suggesting its potential for incorporation in materials for long-term loading applications, such as artificial cartilage.

Received 28th May 2025,  
Accepted 22nd August 2025

DOI: 10.1039/d5lp00156k

rsc.li/rscapplpolym

## Introduction

Poly(vinyl alcohol) (PVA), a synthetic polymer containing abundant hydroxyl groups, is widely used in a range of applications, including in the textile industry, polarising plates, food packaging films, and tissue engineering.<sup>1–5</sup> PVA is known to exhibit a range of desirable characteristics, including a good water solubility, alkali resistance, chemical resistance, and biodegradability.<sup>6–9</sup> In addition, its low toxicity to organisms and its high biocompatibility have led to extensive research into its application as a biomaterial.<sup>10,11</sup> In particular, PVA hydrogel (PVA-H), which is prepared *via* a physical crosslinking approach, is suitable for use as a biomaterial because its preparation does not require the use of toxic crosslinking agents, unlike in the case of chemical crosslinking approaches.<sup>12</sup> Consequently, PVA-H has been used in contact lenses owing to its high transparency and water content.<sup>13</sup> This material has also been employed as a cell scaffold material in tissue engineering.<sup>5</sup> Additionally, the presence of physical crosslinking imparts PVA-H with an extremely high mechanical strength owing to the formation of microcrystals

through hydrogen bonding. Since the first application of PVA-H in artificial cartilage by Bray *et al.*,<sup>14</sup> extensive studies have been performed in this field. Such applications are of particular interest because PVA-H exhibits mechanical and frictional properties comparable to those of biological articular cartilage, thereby endowing it with a high degree of biocompatibility. However, the majority of PVA-H samples are prepared using the freeze-thaw (FT) method,<sup>15</sup> which generates an opaque and cloudy hydrogel with a low mechanical strength. These characteristics can be attributed to phase separation between the concentrated and diluted layers during ice crystallisation. In addition, other issues, such as melting of the crystallites and over-crystallisation after long periods of time,<sup>16</sup> must be addressed when considering the long-term use of such materials in artificial cartilage.

In this context, Hyon *et al.* prepared clear, high-mechanical-strength PVA-H *via* low-temperature crystallisation (LTC) at  $-20\text{ }^{\circ}\text{C}$  in a mixture of water and dimethyl sulfoxide (DMSO).<sup>17</sup> However, the use of DMSO as an organic solvent during the preparation of PVA-H biomaterials is undesirable. To address this, Sakaguchi *et al.* reported that PVA-H can also be prepared *via* a hot pressing process using water and PVA.<sup>18</sup> Notably, this technology does not require dissolution in water, since gelation can be achieved by simply compressing the product in a swollen state at a high concentration of  $\sim 50\text{ wt\%}$ . Although this material shows promise for use in applications such as

<sup>a</sup>School of Materials Science, Japan Advanced Institute of Science and Technology, 1-1 Asahidai, Nomi, Ishikawa 923-1292, Japan. E-mail: [mkazuaki@jaist.ac.jp](mailto:mkazuaki@jaist.ac.jp)

<sup>b</sup>Organization for Research and Development of Innovative Science and Technology (ORDIST) Kansai University, 3-3-35 Yamate, Suita, Osaka 564-8680, Japan



artificial cartilage, joints and cartilage are subjected to extremely strong loads, and currently, the extent to which PVA-H is resistant to such loads remains unknown.

To date, many high-strength PVA-Hs have been developed using various methods, such as chemical crosslinking, with one example including double network (DN) gels.<sup>19,20</sup> The most commonly used PVA is atactic PVA (aPVA), which exhibits a random arrangement of hydroxyl-bearing side chains and demonstrates a limited crystallinity. Consequently, this material possesses a limited mechanical strength. To address this issue, syndiotactic PVA (sPVA) was developed, which exhibits a higher crystallinity than aPVA. The structure of sPVA consists of side chains and hydroxyl groups that are arranged in an alternate and regular manner relative to the main chain. Although sPVA exhibits a superior mechanical strength and crystallinity compared to aPVA, it is rarely employed due to its poor solubility in water and DMSO, which renders it difficult and impractical to handle. Thus, since gelation cannot be achieved through conventional freezing and thawing, or via low temperature crystallisation, it is not possible to design materials that exhibit these desirable properties.

Although the synthetic approach to sPVA is comparable to that of aPVA, different starting monomers are employed. Additionally, several methods have been reported to improve the syndiotacticity of PVA. For example, Yamada *et al.*<sup>21</sup> and Nagara *et al.*<sup>22</sup> reported that highly syndiotactic PVA can be synthesised *via* the free-radical polymerisation of vinyl acetate (VAc) in a fluoroalcohol solvent. However, due to the steric hindrance caused by neighbouring substituents, vinyl benzoate, vinyl butyrate, and vinyl pivalate (VPi) are often used instead of VAc to prepare sPVA with a higher degree of polymerisation (Scheme 1(a)–(c)).

In this study, an sPVA hydrogel (sPVA-H) is prepared using sPVA (syndiotactic-rich PVA with an atactic structure, produced *via* the free radical polymerisation of VPi) and subsequent saponification (Scheme 1(d)). This is achieved using a hot-pressing method that does not require dissolution of the hydrogel in water, and is expected to produce a high-strength material with a high elastic modulus for use in applications such as artificial cartilage. Following preparation of the desired sPVA-H, heat treatment is performed at several temperatures, and the resulting products are evaluated and com-

pared with an aPVA hydrogel (aPVA-H) in terms of the water content, mechanical strength, and thermophysical properties.

## Experimental

## Materials

The sPVA and aPVA (JF-17 grade) were provided by Japan Vam & Poval Co., Ltd (Osaka, Japan). The sPVA sample exhibited a 1700 degree of polymerisation and 99.0 mol% saponification, while the aPVA sample exhibited a 1700 degree of polymerisation and 98.0–99.0 mol% saponification. DMSO-*d*<sub>6</sub> was purchased from Kanto Chemical Co., Inc. (Tokyo, Japan). Deionised water was used in all experiments.

## Gelation of aPVA and sPVA

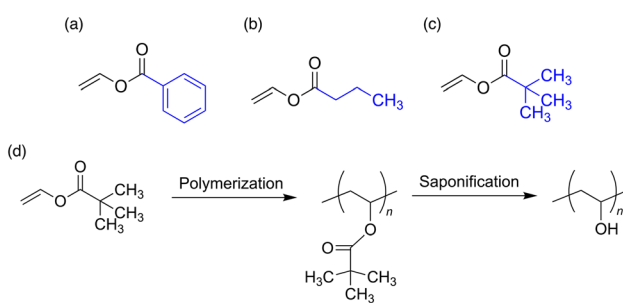
PVA-H was formed using a previously described hot-pressing method.<sup>18</sup> More specifically, aPVA and water were mixed in a 50:50 wt% ratio with stirring, and the aPVA was allowed to swell for 15 min. After this time, the mixture was spread uniformly on a 2 mm-thick mould and hot pressed using a hot press machine (ASONE, Osaka, Japan) at 95 °C. Hot pressing was performed at 2 MPa for 5 min, then at 10 MPa for 10 min, and finally at 20 MPa for 15 min. After removal from the hot press, the product was sealed and allowed to gel at 25 °C for 2 d within the mould. The gel product was then subjected to vacuum drying for 2 d to give the desired aPVA-H. For the gelation of sPVA, sPVA and water were mixed in a 40:60 wt% ratio with efficient stirring, and the sPVA was allowed to swell for 15 min. This ratio was selected because sPVA possesses a high syndiotacticity and molecular weight, resulting in an extremely poor water solubility and limited swelling properties. Consequently, a high moisture content is required during the initial stage to obtain a uniform gel. Subsequently, the mixture was spread uniformly on a 2 mm-thick mould and hot pressed using a hot press machine at 130 °C. All subsequent hot pressing and gelation conditions were as those described for aPVA, and yielded the corresponding sPVA-H. The gelation method is shown in Fig. 1, along with a photographic image of the prepared PVA-Hs.

### Heat treatment and swelling

To increase the sample crystallinity and to obtain both a low water content and favourable mechanical properties, heat treatment of the aPVA-H and sPVA-H samples was performed under vacuum in a vacuum oven (100, 150, or 180 °C for 1 h). The samples heat-treated at 100 °C were denoted as aPVA100 and sPVA100, respectively, while those heat-treated at 150 °C were denoted as aPVA150 and sPVA150, and those heat-treated at 180 °C were denoted as aPVA180 and sPVA180. Following heat treatment, the samples were hydrated in distilled water for 3 d, with the exception of the samples used to perform the dry state measurements.

## Nuclear magnetic resonance spectroscopy

The **[S]-triad (%)** of PVA is an indicator of the polymer syndiotacticity. Thus, proton nuclear magnetic resonance ( $^1\text{H}$  NMR)



**Scheme 1** Vinyl monomers commonly used in the synthesis of sPVA: (a) vinyl benzoate, (b) vinyl butyrate, and (c) vinyl pivalate. (d) Synthesis of sPVA from vinyl pivalate.

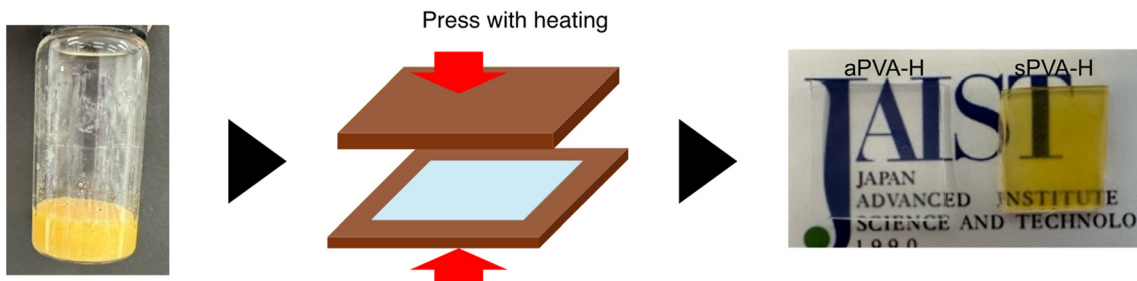


Fig. 1 Gelation of PVA via the hot pressing method.

spectroscopy was used to calculate the tacticity of the [S]-*triad* of PVA, using DMSO-*d*<sub>6</sub> as the solvent. The obtained spectrum exhibited three characteristic peaks corresponding to the [H], [I], and [S] hydroxyl protons at ~4–5 ppm. The peak appearing at the lowest field indicates the presence of an isotactic [I] sequence, while the middle peak corresponds to an atactic (heterotactic) [H] sequence, and the peak appearing at the highest magnetic field represents a syndiotactic [S] sequence. Thus, the [S]-*triad* (%) was calculated using eqn. (1) based on the integral ratio of each hydroxyl proton signal.<sup>23,24</sup>

$$[\text{S}]\text{-triad} (\%) = \frac{[\text{S}]}{[\text{I}] + [\text{H}] + [\text{S}]} \times 100 \quad (1)$$

#### Measurement of the water content

The water contents of the aPVA-H and sPVA-H specimens were measured by hydrating the dry PVA-H for 3 d at 25 °C. The water content  $W_c$  (%) was subsequently calculated using eqn (2):

$$W_c (\%) = \frac{W_{\text{wet}} - W_{\text{dry}}}{W_{\text{wet}}} \times 100 \quad (2)$$

where  $W_{\text{wet}}$  is the weight of PVA-H in the hydrated state and  $W_{\text{dry}}$  is the weight of PVA-H in the dry state.

#### Fourier transform infrared spectroscopy

Fourier transform infrared (FT-IR) spectroscopy was performed using the attenuated total reflection (ATR) mode with an FT/IR 4× instrument (JASCO, Tokyo, Japan). All spectra were obtained by scanning 16 times over a measurement range of 4000–400 cm<sup>-1</sup> with a resolution of 4 cm<sup>-1</sup>. Subsequently, the crystallinity ( $X_c$ , %) of PVA-H was calculated using eqn (3), as reported previously by Tretinnikov *et al.*<sup>25</sup>

$$X_c (\%) = -13.1 + 89.5 \left( \frac{A_{1144}}{A_{1094}} \right) \quad (3)$$

where  $A_{1144}$  is the absorbance at 1144 cm<sup>-1</sup>, and  $A_{1094}$  is the absorbance at 1094 cm<sup>-1</sup>.

#### Differential scanning calorimetry

The melting points of aPVA-H and sPVA-H in the dry state were determined by differential scanning calorimetry (DSC; Discovery DSC2500, TA Instruments, Delaware, USA). For this

purpose, dried PVA-H (5–10 mg) was placed in an aluminium pan and sealed. An empty aluminium pan was used as the reference material and scanning was performed over a temperature range of 0–300 °C at a rate of 5 °C min<sup>-1</sup>. All measurements were performed under a nitrogen atmosphere.

#### Tensile tests

Tensile tests were performed for the hydrated aPVA-H and sPVA-H specimens using an Autograph AGS-J system (Shimadzu Corporation, Kyoto, Japan) fitted with a 100 N load cell in a water tank. The material was elongated at a rate of 5 mm min<sup>-1</sup> until reaching failure. The Young's modulus was calculated based on Hooke's law from a crinkle between 0.1 and 0.5 mm. Three measurements were taken for each sample, and the average value was calculated.

#### Wide-angle X-ray diffraction

Wide-angle X-ray diffraction (WAXD) measurements were performed using a Smart Lab X-ray diffractometer (Rigaku, Tokyo, Japan) to analyse the number of crystals in the dried PVA-H sample. CuK $\alpha$  rays were generated at a voltage of 45 kV and a current of 200 mA, and the irradiation time was set at 5 min. The camera length was 27 mm and the X-ray transmission width was 2 mm. All samples were irradiated along the cross-sectional direction of the hydrogel.

#### Statistical analysis

All data are expressed as the mean  $\pm$  standard deviation (SD). All experiments were conducted for  $N = 3$ . Ordinary two-way analysis of variance combined with Tukey's multiple comparison test was used for data comparison. Differences were considered statistically significant at  $P < 0.05$ .

## Results and discussion

#### Calculation of syndiotacticity using <sup>1</sup>H NMR spectroscopy

Fig. 2(a) and (b) show the <sup>1</sup>H NMR spectra of the prepared aPVA and s-PVA materials. Generally, when water is used as the solvent for <sup>1</sup>H NMR spectroscopy, rapid proton exchange occurs, thereby hindering measurement of the hydroxyl groups. In contrast, the use of DMSO-*d*<sub>6</sub> as the solvent suppresses proton exchange, leading to the observation of three



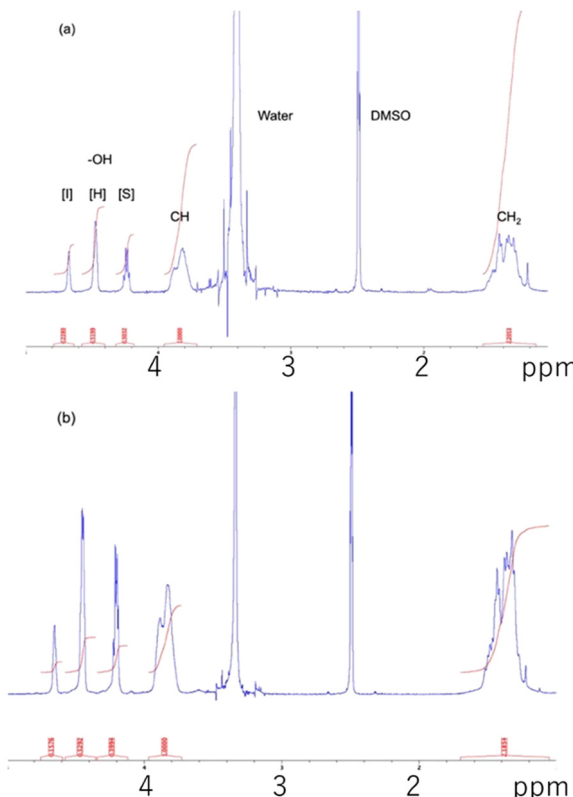


Fig. 2  $^1\text{H}$  NMR spectra of the (a) aPVA and (b) sPVA specimens in  $\text{DMSO}-d_6$ .

characteristic peaks corresponding to the [I], [H], and [S] hydroxyl group protons at 4.0–5.0 ppm.<sup>23,24</sup> The peaks split in this manner because the chemical shifts of the hydroxyl protons are affected by the spatial arrangement (tacticity) of the adjacent carbon atoms. Using the integrated values of these three peaks, the [S]-*triad*, which is an indicator of PVA syndiotacticity, can be calculated. Thus, the [S]-*triad* values calculated herein for the aPVA and sPVA species were 28.8 and 36.8%, respectively.

#### Measurement of the hydrogel water content

Fig. 3 shows the results of the water content measurements for the various hydrogel samples, wherein it can be seen that under all heat-treatment conditions employed herein, the water content of sPVA-H was lower than that of aPVA-H. For example, following heat treatment at 100 °C, the water content of aPVA-H was 60.0%, while that of sPVA-H was 36.5%, representing an almost two-fold difference at the same heat treatment temperature. Overall, the water content of aPVA-H decreased upon increasing the heat-treatment temperature. For the sPVA-H system, the water content decreased only slightly from 36.5 to 29.6% upon increasing the heat treatment temperature from 100 to 150 °C, and upon increasing the temperature further to 180 °C, only a small reduction was observed. This effect may be due to the structure of sPVA-H, which crystallises more easily under heat treatment con-

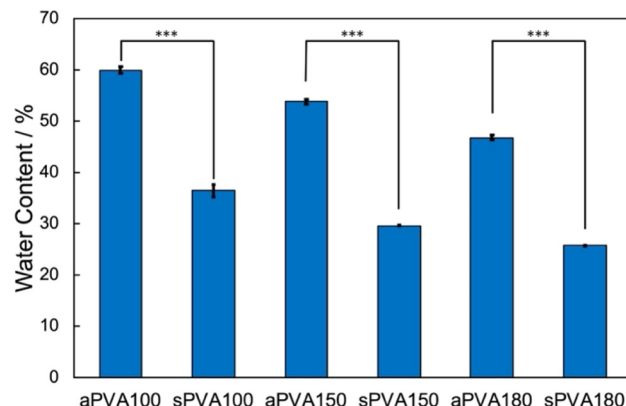


Fig. 3 Water contents of the aPVA-H and sPVA-H specimens subjected to heat treatment at different temperatures. \*\*\* $P < 0.001$ .

ditions, thereby suggesting that its water content can be controlled using lower heat treatment temperatures or shorter times than those required for aPVA-H. Additionally, the low water content of the sPVA-H sample was attributed to its high tacticity, which facilitated crystallisation through the formation of hydrogen bonds between the regularly arranged hydroxyl groups.<sup>26</sup> Notably, highly crystallised PVA is known to exhibit a low water content owing to its weaker interactions with water. Moreover, the low water content of the PVA-H prepared using the hot-press method was partly attributed to the higher initial concentration of PVA compared to that present in the LTC system, resulting in a higher molecular density and more facile crystallisation.<sup>18</sup>

#### FT-IR spectroscopy

The structures of semi-crystalline polymers, such as PVA, can be characterised based on the degree of crystallinity, which is related to the molecular motion of the crystalline and amorphous hydroxyl groups that are linked through intermolecular interactions. In the obtained FT-IR spectra, an absorption band with a maximum at 1094  $\text{cm}^{-1}$  was observed, which was attributed to overlap of the bands corresponding to the C–O stretching vibrations of the C–OH groups and a band with a maximum at 1144  $\text{cm}^{-1}$ , which corresponded to the crystallisation of PVA. As previously reported, the intensity of the band at 1144  $\text{cm}^{-1}$  increases with an increasing PVA crystallinity.<sup>27,28</sup> Thus, as described by Tretinnikov *et al.*,<sup>25</sup> these effects allow the use of FT-IR spectroscopy to calculate the crystallinity of any PVA sample. For the purpose of this study, the spectra recorded between 3000–3600 and 1000–1200  $\text{cm}^{-1}$  were evaluated for determination of the crystallinity. More specifically, Fig. 4(a) shows the FT-IR spectra recorded for the various aPVA-H and sPVA-H samples; the corresponding enlargements are presented in Fig. 4(b) and (c). Considering the bands corresponding to the stretching vibrations of the PVA hydroxyl groups, it was observed that the most intense peak for the sPVA-H sample was shifted to a higher frequency than that of the aPVA-H specimen. In addition, in the crystallisation band



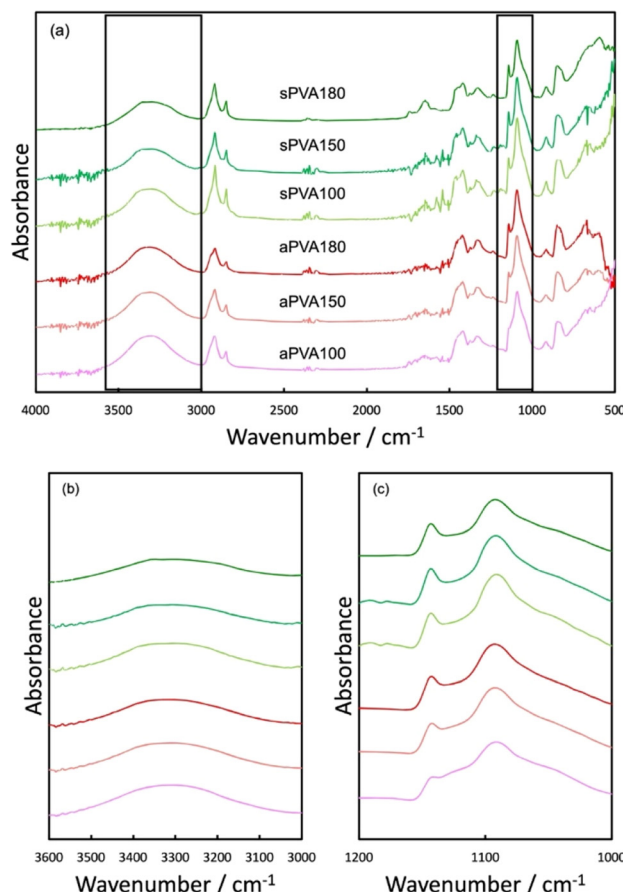


**Fig. 4** FT-IR spectra recorded for the aPVA-H and sPVA-H species. (a) The full scanning range, (b) magnification of the  $3000\text{--}3600\text{ cm}^{-1}$  range, and (c) magnification of the  $1000\text{--}1200\text{ cm}^{-1}$  range.

at  $1144\text{ cm}^{-1}$  a higher peak intensity was observed for the sPVA-H sample, thereby indicating that the sPVA-H system contained a greater amount of crystallised polymer (*cf.*, aPVA-H).

The crystallinity results calculated from the FT-IR spectra are presented in Fig. 5 and Table 1, wherein it is evident that the sPVA-H system generally exhibited a higher degree of crystallinity than the aPVA-H sample. In addition, these results confirm that the degree of crystallinity increased with an increasing heat treatment temperature. Although the heat treatment approach is often used to increase the crystallinity of a polymer such as PVA, it is noteworthy that when employing the same heat treatment temperature, a higher degree of crystallinity was observed for sPVA-H. This indicated that sPVA crystallised more easily than aPVA. Interestingly, the crystallinity of aPVA180 was comparable to that of sPVA100, thereby suggesting that sPVA can achieve a high degree of crystallinity even upon heat treatment at relatively low temperatures. Moreover, the obtained results indicate that the heat treatment of sPVA-H at  $\geq 150\text{ }^{\circ}\text{C}$  yields PVA-H specimens with crystallinities of  $\geq 50\%$ . Overall, the presence of a greater number of crystalline species in the sPVA-H specimen indicates the generation of stronger crosslinked structures.

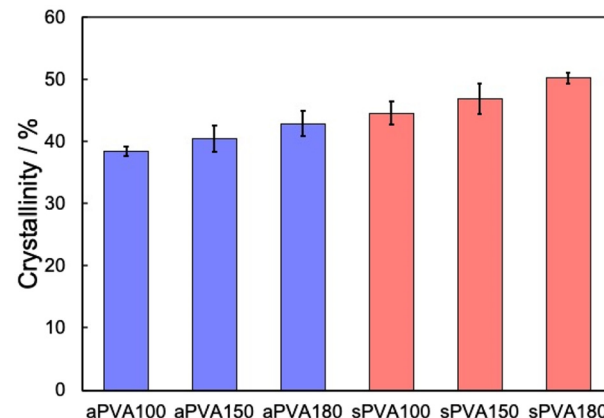


**Fig. 5** Comparison of the sample crystallinity values (%) calculated from the FT-IR spectra.

**Table 1** Crystallinity values (%) calculated from the FT-IR spectra ( $\pm$  standard deviation)

Sample	Crystallinity/%
aPVA100	$38.4 \pm 0.8$
aPVA150	$40.4 \pm 2.1$
aPVA180	$42.9 \pm 2.1$
sPVA100	$44.6 \pm 1.9$
sPVA150	$46.9 \pm 2.5$
sPVA180	$50.2 \pm 0.8$

### DSC measurements

Fig. 6(a) and (b) show the DSC heating curves recorded for the dry aPVA-H and sPVA-H specimens, respectively. From these curves, it can be seen that the melting point of sPVA-H is  $>20\text{ }^{\circ}\text{C}$  higher than that of aPVA-H, thereby suggesting a change in the crystal structure, along with an increase in the lamellar crystal thickness in the former specimen. Since the melting point of aPVA100 is close to the melting point reported for PVA, it was considered that in the case of aPVA, no change in the crystal structure occurred after heat treatment at  $100\text{ }^{\circ}\text{C}$ .<sup>29</sup> However, the melting point of sPVA100 reached  $248.8\text{ }^{\circ}\text{C}$ , implying more facile crystallisation. Although the melting point of the aPVA-H sample increased with an increasing heat treatment temperature, the melting point of sPVA-H remained relatively constant, implying the formation of high-melting-point crystals in the sPVA-H system. Thus, although heat treatment causes a change in the degree of crystallinity, the crystal structure itself appeared to show little variation (see the WXRD results for further details). In the case of the aPVA-H system, it can be inferred that high-melting-point crystals were also generated following heat treatment. Furthermore, the DSC heating curve showed an interesting change, wherein the melting peak of aPVA appeared as a split peak, whereas a clear single peak appeared for sPVA. This was likely due to the fact that aPVA exhibits similar melting and decomposition temperatures, which results in the two processes occurring simultaneously. On the other hand, for the sPVA system, it was proposed that the

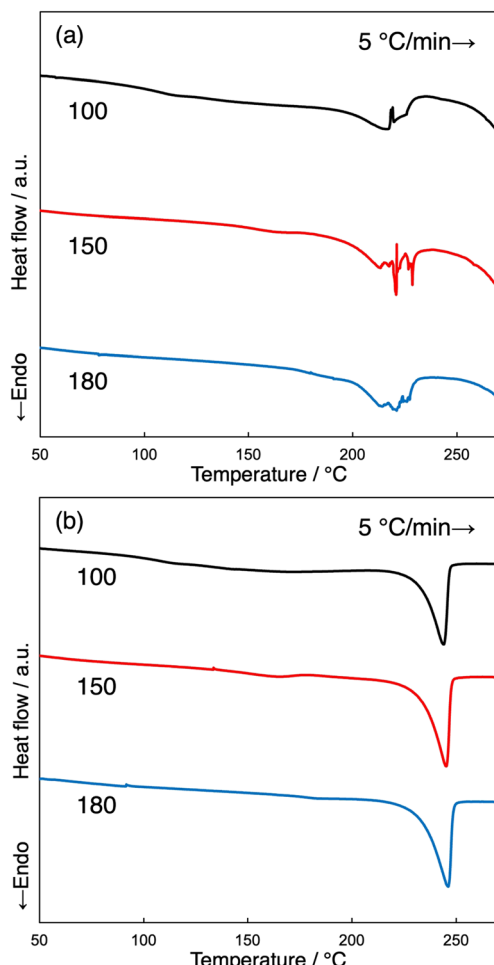


Fig. 6 DSC heating curves recorded for the (a) aPVA-H and (b) sPVA-H specimens.

decomposition temperature may have increased along with the melting temperature, consistent with a study by Wang *et al.*,<sup>30</sup> who found that the decomposition temperature of fibres spun using sPVA increased.<sup>30</sup> Considering that the decomposition temperature of sPVA is higher than its melting point, it was therefore considered that decomposition and melting did not occur simultaneously, ultimately leading to a distinct peak for each process.

#### Tensile tests for measurement of the Young's modulus

Fig. 7 shows the Young's moduli obtained from the tensile tests. Compared with aPVA-H, sPVA-H exhibited a higher Young's modulus, even following lower heat treatment temperatures. Among the various samples, sPVA180 exhibited the highest Young's modulus of 58.8 MPa, which is significantly higher than that of aPVA180. Notably, even in the case of the aPVA180, which represented the aPVA specimen subjected to the highest heat treatment temperature, the Young's modulus remained lower than that of the sPVA100 specimen. These results indicated that sPVA-H exhibits superior mechanical properties compared to aPVA-H, wherein the Young's modulus

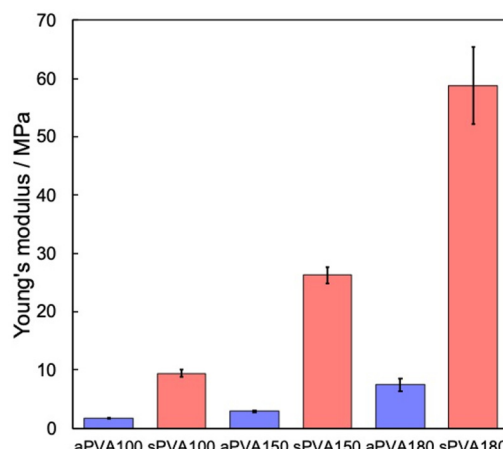


Fig. 7 Determination of the Young's modulus via tensile testing.

of the former improved to a greater extent upon increasing the heat treatment temperature. The effect of this improvement was significantly greater than that observed for aPVA-H, and as a result, it was not possible to achieve a high Young's modulus for the aPVA-H specimen. However, although sPVA-H exhibits a high Young's modulus, the amount of strain is extremely small, resulting in a hard and brittle gel (Fig. S1). This could possibly be addressed by increasing the temperature and duration of water impregnation; however, in this case, there is also concern regarding a decrease in the Young's modulus. Further tuning of the Young's modulus of sPVA-H may therefore be required by changing the temperature and duration of the heat treatment process. Moreover, it was found that between the sPVA100 and aPVA180 samples, which contained similar water contents, sPVA100 exhibited a higher elastic modulus. This can be attributed to the fact that sPVA-H easily crystallises at low heat treatment temperatures owing to its excellent tacticity.

#### WAXD

Fig. 8 shows the WAXD plots obtained for the dry aPVA-H and sPVA-H specimens following heat treatment. For crystalline PVA, a maximum peak corresponding to the  $[10\bar{1}]$  plane should be observed at  $19.4^\circ$  ( $4.68\text{ \AA}$ ) along with a sharp crystalline reflection peak with a shoulder at  $20^\circ$  ( $4.43\text{ \AA}$ ), which corresponds to the  $[101]$  plane.<sup>31</sup> In addition, the intensity of the peak at  $19.4^\circ$  is known to depend on the amount of crystalline PVA, while a broad peak indicates an amorphous state. The intensities of these characteristic peaks increase in the presence of abundant crystals, and so the clear peaks observed for both aPVA-H and sPVA-H suggest that both specimens exhibit high degrees of crystallinity. In particular, the strongest peak intensity was observed for sPVA180, indicating that this specimen contained more abundant crystals than the other hydrogels. However, the comparable diffraction patterns observed for aPVA and sPVA suggest that their crystal structures were almost identical.<sup>26</sup> In the future, further investigations into the crystal size distribution are required based on X-ray



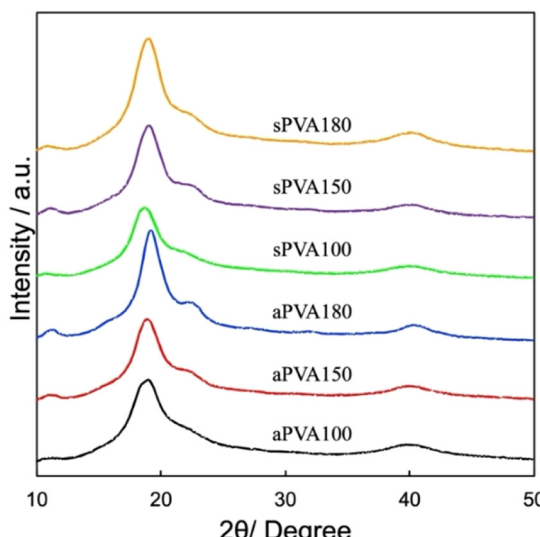


Fig. 8 WAXD profiles of the various aPVA-H and sPVA-H specimens.

scattering and neutron scattering methods. Such investigations would be expected to further deepen our understanding of sPVA-H.

## Conclusions

In the present study, the gelation of syndiotactic-rich polyvinyl alcohol (sPVA) was performed using hot pressing, which represents an organic solvent-free approach to this structure. More specifically, hot pressing was considered to be a superior route to the gelation of sPVA because it does not require dissolution of the largely insoluble polymer in water. Notably, the prepared sPVA hydrogel (sPVA-H) exhibited a higher crystallinity, a lower water content, and a higher Young's modulus than the commonly employed atactic PVA (aPVA), even under comparable heat treatment conditions. Consequently, sPVA-H demonstrated superior mechanical properties to aPVA-H, despite the fact that both hydrogels were prepared using an identical approach. This was attributed to the superior tacticity (syndiotacticity) of sPVA compared to that of aPVA. Since the gelation of sPVA is not possible using standard solvent-based approaches due to its insoluble nature, gelation by hot pressing addresses this issue, producing gels with a high degree of crystallinity. It is therefore expected that the developed sPVA-H will be suitable for use as an alternative for artificial cartilage, in addition to other biomaterials that require a high material strength.

## Author contributions

Conceptualisation: Y. T. and K. M., methodology: Y. T. and K. M., funding acquisition: K. M., investigation: Y. T., formal analysis: Y. T. and K. M., writing – original draft: Y. T., writing – review & editing: Y. T. and K. M.

## Conflicts of interest

There are no conflicts to declare.

## Data availability

The data supporting this article have been included as part of the SI. See DOI: <https://doi.org/10.1039/d5lp00156k>.

## Acknowledgements

The authors would like to express their deepest gratitude to Japan VAN & POVAL Co., Ltd for synthesising and providing the aPVA and sPVA samples.

## References

- 1 C. C. DeMerlis and D. R. Schoneker, Review of the oral toxicity of polyvinyl alcohol (PVA), *Food Chem. Toxicol.*, 2003, **41**(3), 319–326.
- 2 J. Ma, X. Ye and B. Jin, Structure and application of polarizer film for thin-film-transistor liquid crystal displays, *Displays*, 2011, **32**(2), 49–57.
- 3 A. A. Oun, G. H. Shin, J. W. Rhim and J. T. Kim, Recent advances in polyvinyl alcohol-based composite films and their applications in food packaging, *Food Packag. Shelf Life*, 2022, **34**, 100991.
- 4 Y. Liu, S. Wang and W. Lan, Fabrication of antibacterial chitosan-PVA blended film using electrospray technique for food packaging applications, *Int. J. Biol. Macromol.*, 2018, **107**(Part A), 848–854.
- 5 A. Karimi and M. Navidbakhsh, Mechanical properties of PVA material for tissue engineering applications, *Mater. Technol.*, 2014, **29**(2), 90–100.
- 6 E. Chiellini, A. Corti, S. D'Antone and R. Solaro, Biodegradation of poly (vinyl alcohol) based materials, *Prog. Polym. Sci.*, 2003, **28**(6), 963–1014.
- 7 T. S. Gaaz, A. B. Sulong, M. N. Akhtar, A. A. H. Kadhumj, A. B. Mohamad and A. A. Al-Amiry, Properties and Applications of Polyvinyl Alcohol, Halloysite Nanotubes and Their Nanocomposites, *Molecules*, 2015, **29**(12), 22833–22847.
- 8 M. Aslam, M. A. Kalyar and Z. A. Raza, Polyvinyl alcohol: A review of research status and use of polyvinyl alcohol based nanocomposites, *Polym. Eng. Sci.*, 2018, **58**(12), 2119–2132.
- 9 N. B. Halima, Poly(vinyl alcohol): review of its promising applications and insights into biodegradation, *RSC Adv.*, 2016, **6**, 39823–39832.
- 10 M. I. Baker, S. P. Walsh, Z. Schwartz and B. D. Boyan, A review of polyvinyl alcohol and its uses in cartilage and orthopedic applications, *J. Biomed. Mater. Res., Part B*, 2012, **100B**(5), 1451–1457.



11 M. Teodorescu, M. Bercea and S. Morariu, Biomaterials of Poly(vinyl alcohol) and Natural Polymers, *Polym. Rev.*, 2018, **58**(2), 247–287.

12 M. H. Alves, B. E. B. Jansen, A. A. A. Smith and A. N. Zelikin, Poly(Vinyl Alcohol) Physical Hydrogels: New Vista on a Long Serving Biomaterial, *Macromol. Biosci.*, 2011, **11**(10), 1293–1313.

13 P. Yusong, D. Jie, C. Yan and S. Qianqian, Study on mechanical and optical properties of poly(vinyl alcohol) hydrogel used as soft contact lens, *Mater. Technol.*, 2016, **31**(5), 266–273.

14 J. C. Bray and E. W. Merrill, Poly(vinyl alcohol) hydrogels for synthetic articular cartilage material, *J. Biomed. Mater. Res.*, 1973, **7**(5), 421–443.

15 H. Adelnia, R. Ensandoost, S. S. Moonshi, J. N. Gavgani, E. I. Vasafi and H. T. Ta, Freeze/thawed polyvinyl alcohol hydrogels: Present, past and future, *Eur. Polym. J.*, 2022, **164**(5), 110974.

16 C. M. Hassan and N. A. Peppas, Structure and Morphology of Freeze/Thawed PVA Hydrogels, *Macromolecules*, 2000, **33**(7), 2472–2479.

17 S. H. Hyon, W. I. Cha and Y. Ikeda, Preparation of transparent poly(vinyl alcohol) hydrogel, *Polym. Bull.*, 1989, **22**, 119–122.

18 T. Sakaguchi, S. Nagano, M. Hara, S.-H. Hyon, M. Patel and K. Matsumura, Facile preparation of transparent poly(vinyl alcohol) hydrogels with uniform microcrystalline structure by hot-pressing without using organic solvents, *Polym. J.*, 2017, **49**, 535–542.

19 Y. Zhang, M. Somg, Y. Diao, B. Li, L. Shi and R. Ran, Preparation and properties of polyacrylamide/polyvinyl alcohol physical double network hydrogel, *RSC Adv.*, 2016, **6**(113), 112468–112476.

20 B. Hou, X. Li, M. Yan and O. Wang, High strength and toughness poly (vinyl alcohol)/gelatin double network hydrogel fabricated via Hofmeister effect for polymer electrolyte, *Eur. Polym. J.*, 2023, **185**(17), 111826.

21 K. Yamada, T. Nakano and Y. Okamoto, Stereospecific polymerization of vinyl acetate in fluoroalcohols Synthesis of syndiotactic poly(vinyl alcohol), *Proc. Jpn. Acad., Ser. B*, 1998, **74**(3), 46–49.

22 Y. Nagara, K. Yamada, T. Nakano and Y. Okamoto, Stereospecific Polymerization of Vinyl Acetate in Fluoroalcohols and Synthesis of Syndiotactic Poly(vinyl alcohol), *Polym. J.*, 2001, **33**, 534–539.

23 T. Moritani, I. Kuruma, K. Shibatani and Y. Fijiwara, Tacticity of Poly(vinyl alcohol) Studied by Nuclear Magnetic Resonance of Hydroxyl Protons, *Macromolecules*, 1972, **5**(5), 577–580.

24 T. K. Wu and D. W. Ovalle, Protone and Carbon-13 Nuclear Magnetic Resonance Studies of Poly(vinyl alcohol), *Macromolecules*, 1973, **6**(4), 582–584.

25 O. N. Tretinnikov and S. A. Zagorskaya, Determination of the degree of crystallinity of poly(vinyl alcohol) by FTIR spectroscopy, *J. Appl. Spectrosc.*, 2012, **79**(4), 521–526.

26 Y. Nagara, T. Nakano, Y. Okamoto, Y. Gotoh and M. Nagura, Properties of highly syndiotactic poly(vinyl alcohol), *Polymer*, 2001, **42**(24), 9679–9686.

27 S. A. Zagorskaya and O. N. Tretinnikov, Infrared Spectra and Structure of Solid Polymer Electrolytes Based on Poly (vinyl alcohol) and Lithium Halides, *Polym. Sci., Ser. A*, 2019, **61**, 21–28.

28 H. Tadokoro, S. Seki and I. Nitta, The Crystallinity of Solid High Polymers. I. The Crystallinity of Polyvinyl alcohol Film, *Bull. Chem. Soc. Jpn.*, 1955, **28**(8), 559–564.

29 R. K. Tubbs, Melting point and heat of fusion of poly(vinyl alcohol), *J. Polym. Sci., Part A: Gen. Pap.*, 1965, **3**(12), 4181–4189.

30 H. Wang, J. He, L. Zou, C. Wang and Y. Wang, Synthesis of syndiotacticity-rich high polymerization degree PVA polymers with Vac and VPa, fabrication of PVA fibers with superior mechanical properties by wet spinning, *J. Polym. Res.*, 2021, **28**, 386.

31 R. Ricciardi, F. Auriemma, C. D. Rosa and F. Lauprêtre, X-ray Diffraction Analysis of Poly(vinyl alcohol) Hydrogels, Obtained by Freezing and Thawing Techniques, *Macromolecules*, 2004, **37**(5), 1921–1927.

